Kufa Journal of Engineering Vol. 16, No. 2, April 2025, P.P. 295 -313 Article history: Received 16 July 2024, last revised 4 September 2024, accepted 13 October 2024



MODELING AND ANALYSIS OF DROP SIZE IN A MODIFIED SPRAY COLUMN FOR AROMATICS EXTRACTION

Marwa Asad Salih^{1,2,*} and Raghad F. Almilly³

- ¹ Department of Chemical Engineering, College of Engineering, University of Kufa, Najaf, Iraq. E-mail: marwa.salih@uokufa.edu.iq
- ² Department of Chemical Engineering, College of Engineering, University of Baghdad, Baghdad, Iraq. E-mail: marwa.salih1507d@coeng.uobaghdad.edu.iq
- ³ Department of Chemical Engineering, College of Engineering, University of Bagdad, Baghdad, Iraq. E-mail: raghad.fareed@coeng.uobaghdad.edu.iq;
- * Corresponding author: marwa.salih1507d@coeng.uobaghdad.edu.iq; ORCID: https://orcid.org/0000-0001-9723-4855

https://doi.org/10.30572/2018/KJE/160218

ABSTRACT

Aromatic compounds are considered the building block for petrochemical industries. In this study, a new pilot-scale counter-current modified spray column was designed and constructed for extracting aromatic compounds from reformate-heavy naphtha (RHN) using furfural as solvent. RHN and furfural were provided by Al-Dora Refinery in Iraq. The new design included a rotor added to the conventional spray column. The effects of solvent-feed ratio (S/F) (0.25-2) and rotor speed (0-1000 rpm) were studied. The extraction efficiency and Sauter mean diameter (d32) were investigated experimentally and modeled by dimensional analysis. The experimental results showed that the extraction efficiency varied significantly with rotor speed and S/F ratio recording 96.5% without plate, and 92.5% with plate at 0 rpm rotor speed. The experimental results also showed that d32 values ranged from 0.0025 m to 0.0055 m, corresponding with changes in efficiency. Depending on the experimental results, a correlation was derived for the efficiency and d32 based on the effective dimensionless numbers in the system. The modeling results demonstrated that Reynolds (Re) and Weber We numbers were the most effective dimensionless groups that affected the extraction efficiency and d32 values.



KEYWORDS

New Modified Spray Column, Extraction of Aromatics, Reformate Heavy Naphtha, Dimensional Analysis, Counter–Current Extraction Column.

1. INTRODUCTION

Petrochemicals are chemicals derived from refining petroleum. Olefins and aromatics are essential to petrochemical industries, developed the basis for a wide range of materials like solvents, detergents, and adhesives. Polymers and oligomers used in fibers, plastics, elastomers, gels, resins, and lubricants are based on olefins. Aromatics, with benzene, toluene, and xylenes (BTX), are primarily obtained from by solvent extraction from reformate naphtha from catalytic reforming. Benzene is used in the production dyes and synthetic detergents. Polyurethanes are produced from benzene and toluene. Xylene is key for plastics and synthetic fibers (Matar and Hatch, 2001). Extraction of aromatic compounds from oil fractions enhances the oil's chemical stability and viscosity index, confirming it performs reliably at different temperatures. Liquidliquid extraction (LLE), commonly used to separate two immiscible liquids, often presents challenges. The process becomes tricky when the liquids have similar densities, viscosities, and surface tensions. Impurities like solids or other liquids can also complicate the extraction (Hoseini et al., 2009). Removing aromatic components from oil fractions involves using a suitable solvent, (Ferro et al., 2015). For effective extraction, the solvent must have high capacity and selectivity for aromatic hydrocarbons. These properties vary with temperature and solute composition. Several studies have examined different solvents to find a suitable one for efficiently separating aromatics from oil cuts (Amani et al., 2017; Idrees et al., 2019; Mostafa et al., 2019).

Furfural is widely used solvent in aromatic extraction from oil cuts, due to its exact balance of selectivity and capacity. It efficiently targets aromatic hydrocarbons with the necessary solvent power, making it an excellent choice for this separation process (De Lucas et al., 1993). Unlike other solvents, furfural retains its selectivity even as the temperature increases, making it effective for light and heavy oil cuts (Kumar and Mohan, 2011). Extractors are classified by phases dispersion and countercurrent flow, with main types include mixer-settlers, columns, and centrifugal contactors (Law and Tood, 2008). Equipment like mixer-settlers, packed columns, pulsed columns, and spray columns enhances mass transfer for efficient separation. Industries prefer extraction columns for their stable operation and high stage efficiency. Non-mechanically agitated extractors, such as spray and packed columns, perform well due to larger drop sizes, despite a smaller interfacial area. Mechanically agitated extractors, like rotating disc columns (RDC), achieve high stage efficiency with a larger interfacial area, though their overall performance may be lower (Ghorbanian et al., 2011; Dash and Mohanty, 2019).

Liquid-liquid extraction, a common separation technique in process industries, involves transferring a solute between droplets of one liquid phase and the bulk of another immiscible

liquid phase. Researchers often study the steady movement of droplets to understand these systems better. Spray columns are the simplest liquid-liquid extraction columns (Salimi-Khorshidi et al., 2013). Non-mechanically stirred columns are valued for their simplicity, affordability, and versatility. They provide a cost-effective way to test mass transfer models. Spray columns, among the most basic extraction units, manage dispersed phase droplets in three distinct configurations: dispersed, constrained, and compact (Sovilj, 2012).

Varfolomeev et al. (2000), explored the average drop size (d32) and dispersed holdup in spray columns with various packing types: loose, close, and turbulized. Their results enhance the understanding of drop dynamics and holdup, offering important insights for improving industrial extraction processes. An artificial neural network (ANN) effectively modeled the extraction of aromatics from lube oil in a rotating disc contactor (RDC), highlighting its effectiveness in complex chemical processes (Mehrkesh et al., 2011).

A new model was developed to predict the average drop size in a spray extraction column. The study found that the Eotvos number had the most impact on drop size, with a prediction error of 8.1% (Ghorbanian et al., 2011). A novel ionic liquid, N-butyl-N-methyl-2-oxopyrrolidonuim bromide, efficiently extracted benzene, toluene, ethylbenzene, and xylene (BTEX) from reformate in oil refining. The study demonstrated that this ionic liquid had greater extraction efficiency than traditional solvents, providing a sustainable and more effective separating method (Bahadue et al., 2014). A mathematical model examined the extracting of aromatic hydrocarbons from aliphatic compounds using ionic liquids in a rotating disc extractor (RDC). The results indicated that higher solvent flow rate and extraction temperature enhanced dearomatization, while rotor speed had a minimal impact (Toghyani and Rahimi, 2017). Saien and Jafari (2019) reviewed Liquid-liquid extraction utilizing drop technology, incorporating chemical additives such as nanoparticles, salts, and surfactants. Their study provided valued insights into enhancing extraction efficiency and process intensification.

A rotating packed bed utilizing centrifugal force was employed to augment the extraction of hexavalent chromium ions from an aqueous solution, using aliquot-336 as the solvent. This methodology significantly enhanced the overall mass transfer coefficient, attaining an increase of 20-25-times in comparison to conventional packed beds (Karmakar et al., 2020). An existing extraction device was redesigned to overcome high temperature and pressure issues, allowing extraction to be carried out under these process intensification (Sakthithasan et al. 2023). This study focused on enhancing the extraction of aromatics from reformate naphtha using furfural as the solvent. A novel design was introduced by inserting in a conventional spray column for intensifying the contact between dispersed (naphtha) and continuous (furfural) phases based on

drop technology, the motivation align with the current trends of resource conservation, energy-consumption, and environmental sustainability. This work provides a comprehensive experimental and modeling analysis, demonstrating that both Reynolds (Re) and Weber (We) numbers are critical in influencing the extraction efficiency and Sauter mean diameter. The study establishes an exclusive correlation between extraction efficiency and the presence of the rotor, offering critical insights for optimization spray column design in industrial processes.

2. EXPERIMENTAL WORK

2.1. Materials

Reformate naphtha and furfural (98.5% purity) were provided from Al-Dora Refinery with the properties listed in Table 1. The materials were utilized in their original state, without any additional processing.

Table 1. Physical Properties of the materials used in the work

	Density	Viscosity	Molecular Weight
Reformed Heavy Naphtha	0.731 (g/ml)	1.03 cSt	80 to 140 (g/mol)
Furfural	1.155 (g/ml)	2.09 cSt	96.09 g/mol

2.2. Experimental Setup

A schematic flow diagram of the experimental setup is depicted in Fig. 1. The pilot scale of the modified spray column (MSC) is constructed from Perspex, with a diameter and height of 11 cm and 75 cm respectively. This system features two input and two output flow streams, with flow meters installed on both input streams to ensure controlling the flow rates of the two phases. Two digital oil pumps were employed to introduce the phases into the column, and two distributors were strategically positioned within the column. The lower distributor is equipped with a removable rotated perforated plate driven by a DC motor. The rotational speed was precisely controlled using a variable electronic speed regulator, enabling precise adjustment to optimize flow conditions. The removable design allowed for system optimization with or without a perforated plate, providing flexibility to enhance mass transfer efficiency by adjusting drop size distribution and interfacial area for optimal performance under various conditions.

2.3. Distributors

2.3.1. Upper Distributor

A stainless-steel distributor for the continuous phase (furfural) comprises two components: two perforated steel plates, each with a diameter of 11 cm and containing 40 holes of 3 mm in diameter. These plates are connected by (two plates) steel tubes, which are 5 mm in diameter and 5 cm in height. This configuration facilitates the distribution of the continuous phase (furfural solvent) and the discharge of the raffinate phase without mixing between the two phases in the distributor. The details of the upper distributor are shown in Fig. 2.

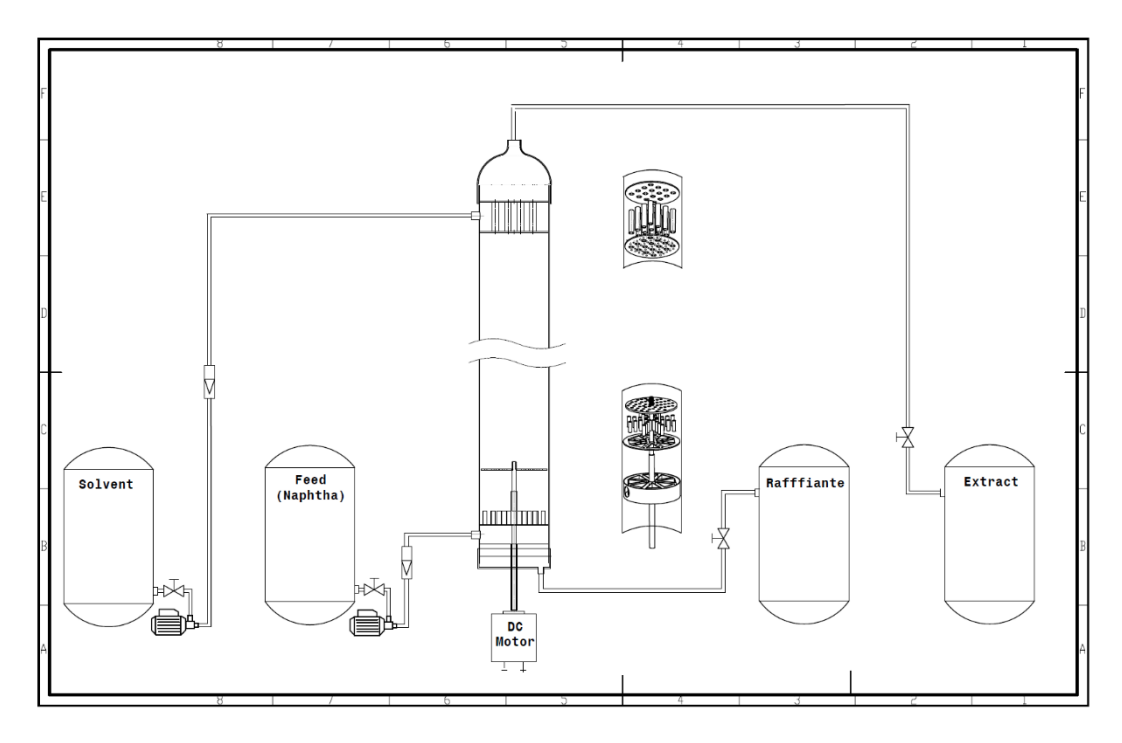


Fig. 1. The Schematic Diagram of Experimental Setup

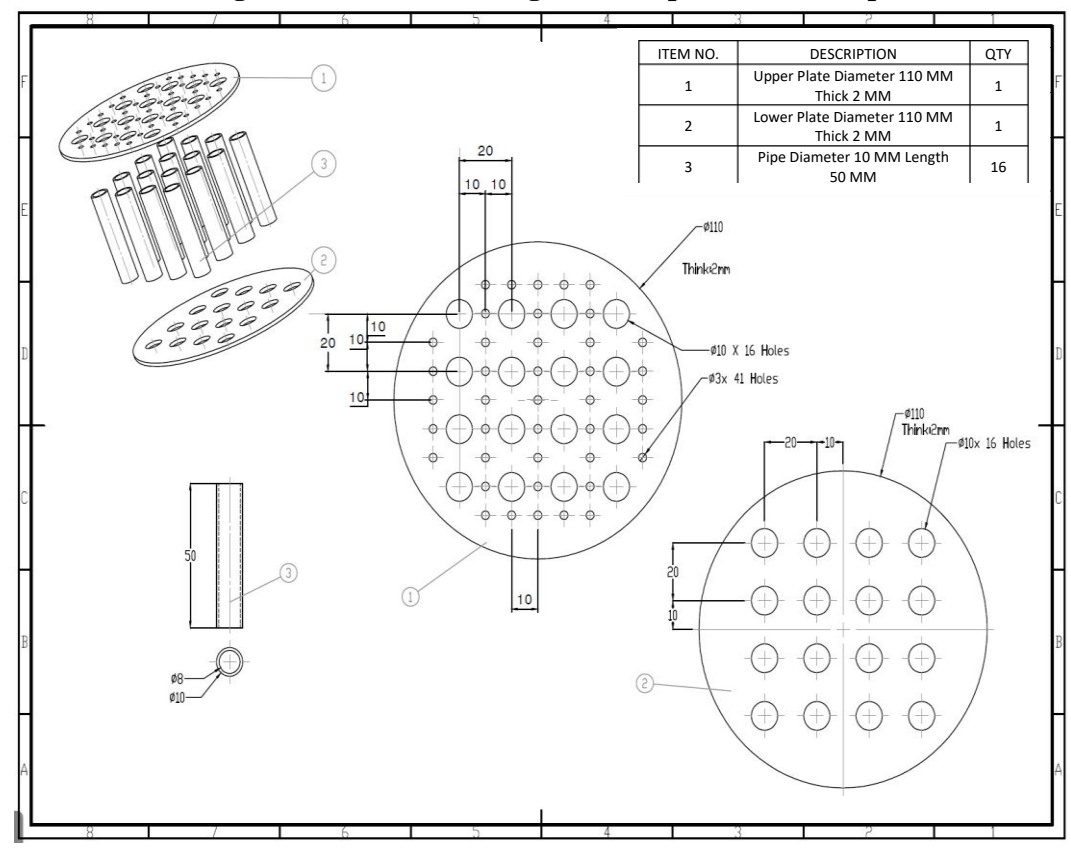


Fig. 2. Details of the Upper Distributor

2.3.2. Lower Distributor

A stainless-steel radial configuration (10.5 cm diameter) distributor has been engineered for the dispersed phase (RHN) at the base of the column. RHN was introduced via a nozzle system, consisting of 16 strategically positioned nozzles, each with a diameter of 3 mm and a length of

2 cm, and radial tubes housing these nozzles. The distributor was equipped with a rotating perforated plate with a diameter of 9.5 cm (40 holes of 3mm diameter) in order to impose turbulence in the rising drops that formed by the nozzles. A stainless-steel shaft, with a diameter of 15 mm and a length of 18 cm, serves as a crucial connecting element, linking the radial configuration and the rotated perforated plate. This shaft is connected to a DC motor via a variable electronic speed regulator, allowing precise control over its rotational speed as shown in Fig. 3. This setup promotes efficient mixing dynamics between the dispersed and continuous phases within the column, enhancing the dispersion process. The direct current (DC) motor provides enhanced control, and the integrated variable electronic speed regulator enables fine-tuned adjustments of the rotational speed, ensuring optimal mixing and interaction between the phases.

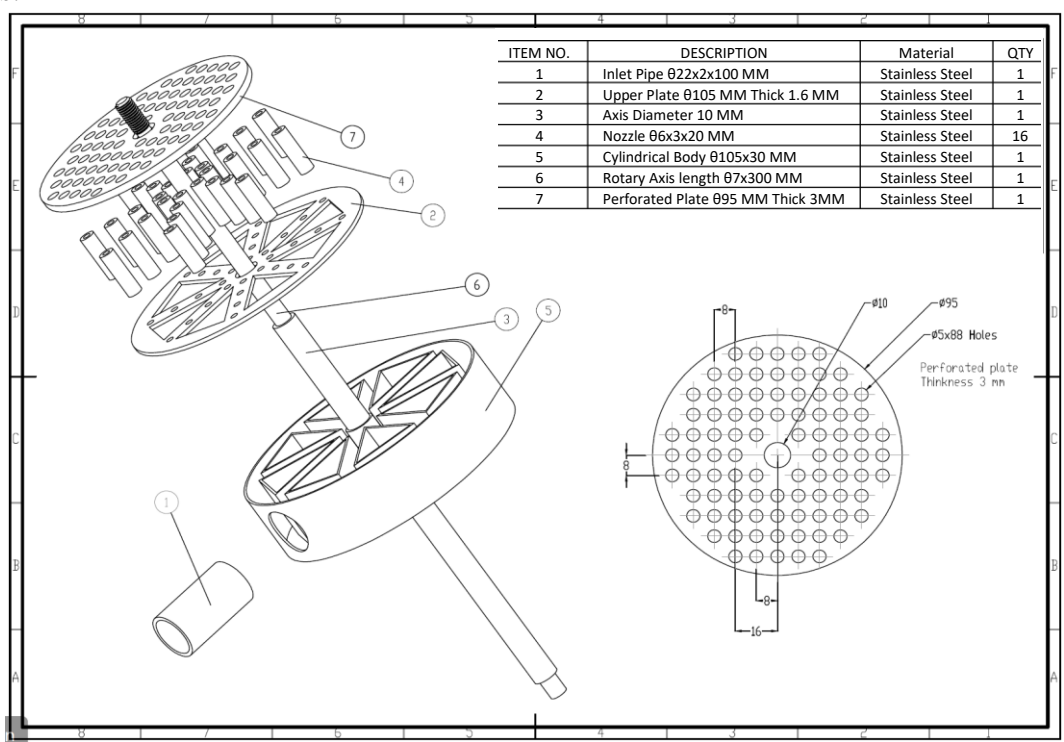


Fig. 3. Details of the Lower Distributor

3. PROCEDURE AND MEASUREMENTS

In this study, the counter-current extraction occurs within a modified spray extractor designed to extract aromatic components from RHN by furfural via solvent extraction. The experiments commenced by pumping RHN from the bottom of the column at different flow rates via the lower distributor which turned RHN to droplets entering the column. Furfural was introduced at the top of the column via the upper distributor with different flow rates. The solvent-to-feed ratio was adjusted in the range (0.25-2) after conducting several trials. In the lower distributor, another variable was introduced to study, the rotor speed in the range (0-1000 rpm). Sixteen experiments were conducted at different S/F ratios and rotor speeds and four experiments were

conducted with removing the rotor installation as shown in Table 2. These variations allowed for a comprehensive analysis of the impact of rotor speed and the presence of the perforated plate on extraction efficiency and the optimization of the design. Throughout each experiment, a Sony A7R IV camera was employed to photograph the droplets along the height of the column. These images were subsequently analyzed using ImageJ software as shown in Fig. 4 to determine the Sauter mean diameters (d32) for each set of photos as in Eq.1. Fig. 4, provide real image of LLE column and the analyzed images at different S/F ratio.

Set No. Solvent/Feed Ratio **Plate Condition** Rotor Speed (rpm) 0.25 (0-250-500-1000)With plate 2 0.5 With plate (0-250-500-1000)3 (0-250-500-1000)With plate 1 4 2 (0-250-500-1000)With plate 5 2 (0-250-500-1000)Without plate

Table 2. Range of variables in experimental work (with and without plate)

$$d32 = \frac{\sum_{i=1}^{N} ni \, di^3}{\sum_{i=1}^{N} ni di^2} \tag{1}$$

Where n: is the number of drops for a specified diameter, d: is the droplet diameter, and N: is the number of all drops.

After the extraction process, the extract was separated into two distinct phases: the upper was rich in naphtha with the aromatics removed, and the lower was rich in furfural-containing aromatics. The aromatic concentrations in various samples were assessed using the PONA test according to ASTM D-3238 (Agilent 7890A Gas Chromatography Device). Also, the surface tension was measured by using a Tensiometer (Sigma 703D).

4. DIMENSIONAL ANALYSIS

The entrainment of the dispersed phase through the continuous phase in the extraction column is a crucial design parameter for characterizing the hydrodynamic behavior and determining the quality of its performance. This study investigates the phenomenon of immiscible liquid entrainment by a liquid jet, which disperses drops by nozzles within the column. Empirical correlations were established using dimensionless parameters to predict extraction efficiency (E%) and Sauter mean diameter (d32). This approach involves a direct use of physical properties and operating variables, to develop more applicable predictions and a new model designed for the modified LLE column.

Based on the experimental data, general correlations using dimensional analysis were suggested which were expressed as a function of the following variables:

$$f(C_{Ri}. C_{Rf}. d32. u_d. \mu_d. \mu_c. \rho_d. \rho_c. d_N. \sigma. g) = 0$$
(2)

Where: C_{Ri} . C_{Rf} are the aromatics concentrations in the raffinate (naphtha) at the inlet and the outlet streams, respectively (mol.L⁻¹), u_d is the dispersed phase (RHN) velocity (m.s⁻¹), μ_d and μ_c are the viscosities of the dispersed and continuous phase, respectively (kg.m⁻¹.s⁻¹), ρ_d and ρ_c are the densities of the dispersed and continuous phase, respectively (kg.m⁻³), d_N is the nozzle diameter (m), σ is the interfacial tension between the two phases (N.m⁻¹), and g is the gravity acceleration (m.s⁻²).

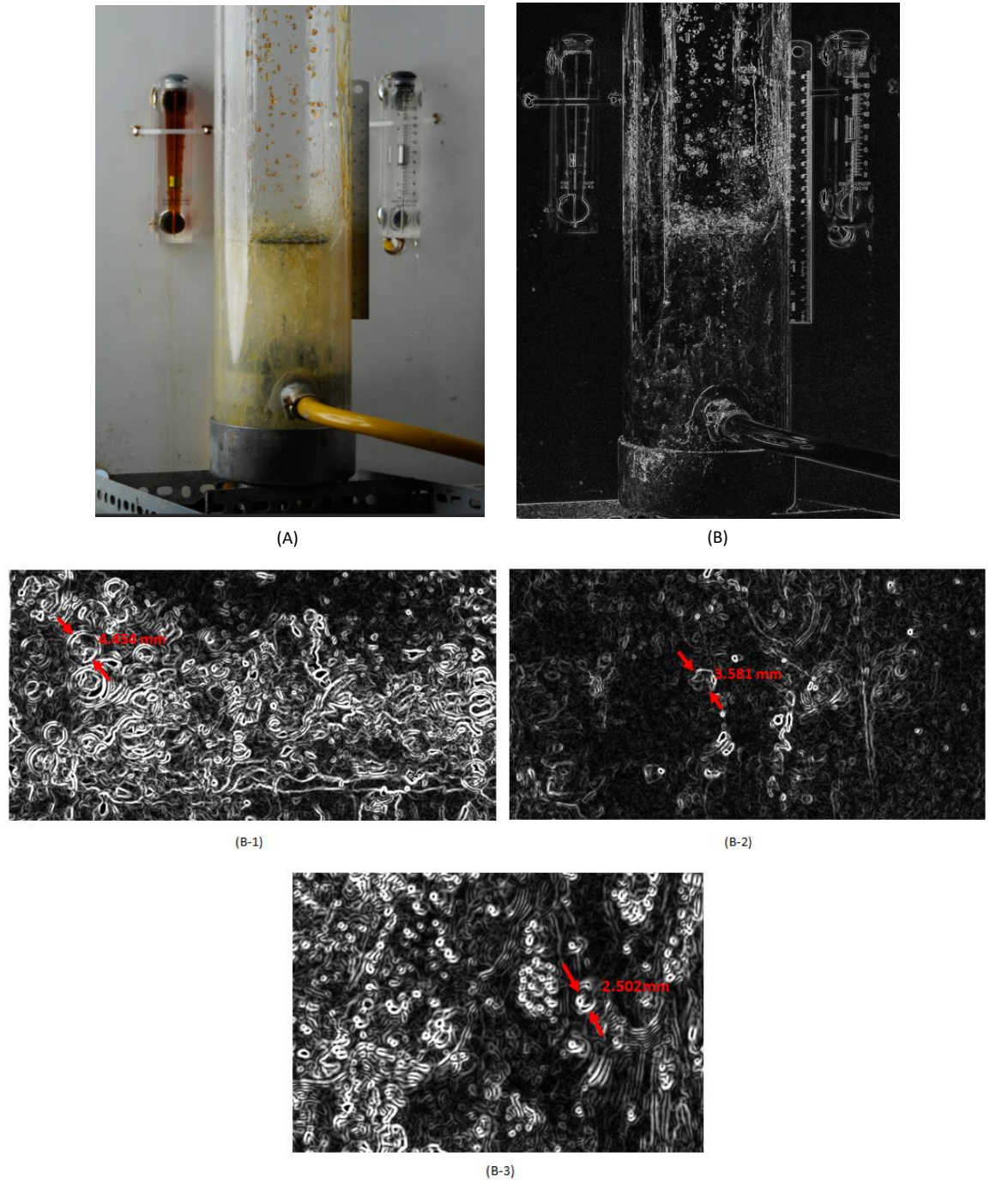


Fig. 4. Drops measurement and analysis: (A) Real image of the column, (B) Analysed image of the column, (B-1) 4.45 mm drop size, (B-2) 3.581 mm drop size, (B-3) 2.502 mm drop size, at different S/F ratio.

Eq. 2 was reformulated using dimensionless groups as follows:

$$f\left(Re.We.E\%.\frac{d32}{d_N}.\frac{\mu_d}{\mu_c}.\frac{\rho_d}{\rho_c}\right) = 0 \tag{3}$$

Where: Re and We are dimensionless Reynolds and Weber numbers, respectively. They are defined as follows:

$$Re = \frac{\rho_d u_d d_N}{\mu_d} \tag{4}$$

$$We = \frac{\rho_d u_d^2 d_N}{\sigma_d} \tag{5}$$

E% is the extraction efficiency which is defined as follows:

$$E\% = \frac{(C_R)_i - (C_R)_f}{(C_R)_i} \times 100\%$$
 (6)

It is a dimensionless value that directly measures the extraction quality. By applying the Buckingham Pi theorem, the following equation was obtained:

$$E\% = C_1 R e^{C2} W e^{C3} (7)$$

This powerful theorem was used to reduce complex physical phenomena by grouping their effect in dimensionless numbers. Similarly to E%, efforts were made in this study to develop an empirical correlation for the Sauter mean diameter d32 in the modified LLE spray column. The correlation for d32 was as follows:

$$\frac{d32}{d_N} = C_1 R e^{C2} W e^{C3} \tag{8}$$

Where C₁, C₂, and C₃ are constants of the two empirical correlations. Later these constants could be obtained from the regression analysis using the least squares method (LSM) to minimize the sum of the squares of the differences between the predicted and the actual values, whereas Excel strong capability in performing LSM analysis, the model were analyzed using this software.

The AARD% is the absolute average relative deviation employed to assess the error between experimental and predicted values for experiment numbers (n) as follows:

$$AARD\% = \left(\frac{1}{n}\sum_{i=1}^{n} \left| \frac{Predicted Y_i - Actual Y_i}{Actual Y_i} \right| \right) *100$$
 (9)

5. RESULTS AND DISCUSSION

5.1. Effect of Solvent-to-Feed Ratio

Fig. 5 shows the extraction efficiency as a function of the S/F ratio at various rotor speeds. It can be observed that the highest efficiency of about 96.5% is achieved at the highest S/F ratio (2) studied in this work. Further increase in the S/F ratio hindered the light phase drops from rising, therefore; shortening the effective length of the column that the two phases contacted

within as it was experienced practically. A higher solvent-to-feed ratio ensures that each drop is surrounded by a sufficient amount of solvent, therefore; improving mass transfer, and extraction efficiency. Nevertheless, increasing the s/f ratio is limited by avoiding wasting solvent and increasing costs. Optimizing the s/f ratio is a key to efficient and economical extraction. This is in agreement with Mahmoudi and Lotfollahi (2010). The amazing observation was that this efficiency was gained with the rotor removed. With the rotor fixed at zero rpm speed, the efficiency dropped to 92.5% at the same S/F ratio. This indicated that the presence of the rotor plate reduced the extraction efficiency even if the S/F ratio was high. The interpretation of this strange result suggests that the rotor plate might hinder the effective contact and mass transfer between the phases by imposing unnecessary turbulence. The absence of the plate might allow a more uniform and less obstructed flow of the phases and enhance overall mass transfer performance. At 250 rpm, the efficiency increased slightly from 65% to 71% as the S/F ratio increased from 0.25 to 2. For 500 rpm and 1000 rpm, the efficiency remained nearly constant with values around 71-72% and 74-75%, respectively, a cross-all S/F ratio.

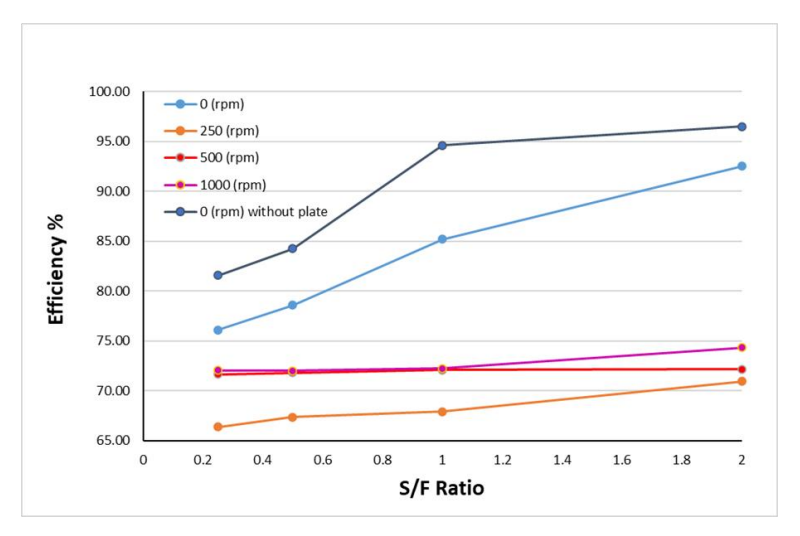


Fig. 5. Extraction Efficiency (E%) vs. S/F Ratio at Different Rotor Speeds

5.2. Effect of Rotor Speed

As shown in Fig. 6, the extraction efficiency generally drops as the rotor speed increases from (0-1000 rpm). This may be due to increased turbulence by high rotation, causing droplets to coalesce reducing mass transfer effectiveness. At higher rotor speeds, efficiency decreases significantly, reaching a low of about 70-75% around 250 rpm. Efficiency then slightly recovers but remains lower than zero-speed value, around 75-80% at 1000 rpm. Higher speeds can also cause back-mixing and increase the number and height of transfer units. Also, increasing rotor speed can lead to more turbulence and higher shear rates which are accompanied by friction causing energy dissipation. This is in agreement with Toghyani and Rahimi (2017).

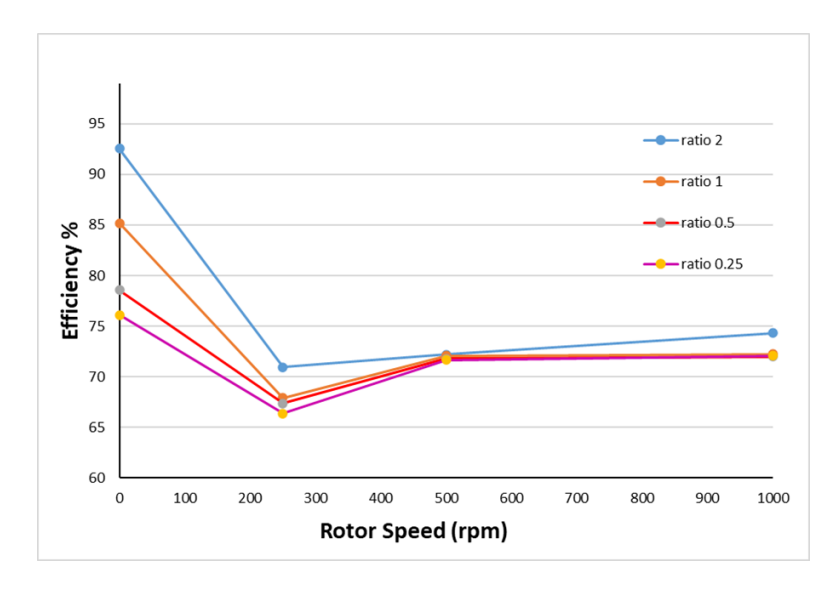


Fig. 6. Extraction Efficiency (E%) vs. Rotor Speed at Different S/F values.

5.3. Effect of Sauter Mean Diameter

Fig. 7 shows the effect of Sauter mean diameter (d32) on the extraction efficiency at different rotational speeds of the rotor. Drop diameter or size is a crucial parameter in the spray extraction column. As drops form through the nozzle, they are subjected to effects determining their age, size, trajectory, and whether they will coalesce with other drops or break up. The Sauter diameter represents the mean diameter that the design and operation of the spray column depend on. By observing the figure, at 0 rpm (i.e. without rotor rotation) the extraction efficiency decreases sharply from around 93% to 80% as d32 increases from 0.0025 m to 0.0055 m. As the rotational speeds increased in the order (250,500, 1000 rpm) the extraction efficiency did not show a significant drop in performance, maintaining around 65-75% even when the drop size increased. This indicates that higher rotational speeds help stabilize the extraction efficiency despite variations in drop size.

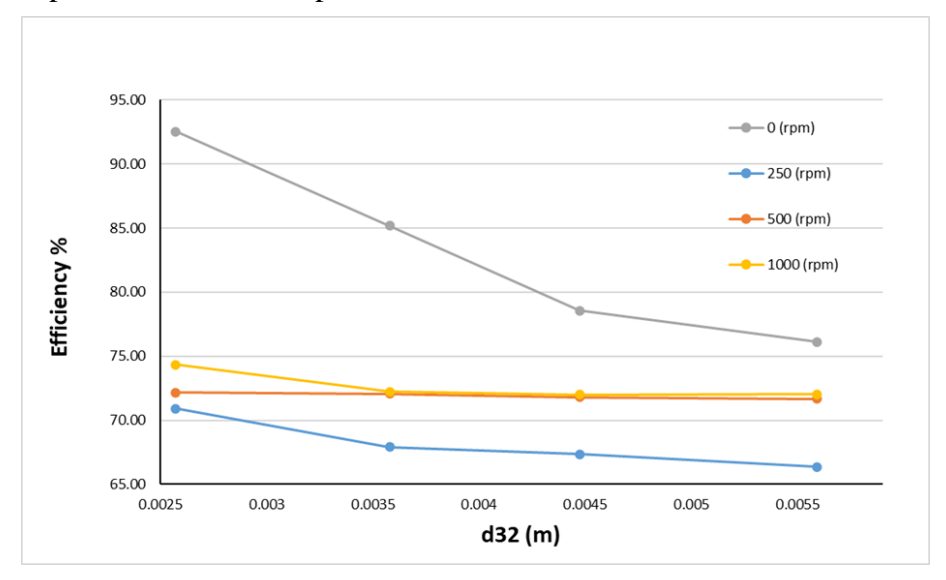


Fig. 7. Extraction Efficiency (E%) vs. d32 at Different Rotor Speeds

5.4. Analyzing Extraction Efficiency Models

Five correlations were suggested to predict the extraction efficiency (E%) in a modified spray column and to represent the actual system. Four of these models took the rotor effect into account, while one did not. Each model showed different coefficients and exponents for Reynolds (Re) and Weber (We) numbers. The models are assessed based on various statistical metrics including R², Adjusted R², Standard Error, t-statistics, P-values, and F-values, as shown in Table 3. The table highlights the performance of various models using parameters like Re and We numbers. Model 4, represented by the equation of efficiency (E%), demonstrated the highest reliability within R² of 0.991, an Adjusted R² 0f 0.975, a standard error of 0.175, and an F-value of 61.39. This model's coefficients showed high statistical significance with a Pvalue of 0.00535 for C1, 0.164 for C2, and 0.116 for C3. In comparison. Model 1, given by E%, had an R² of 0.986 and an R² adj. of 0.960, with a standard error of 1.457 and an F-value of 37.87. Despite its high R², the standard error was larger than that of Model 4, indicating less precision. Models 2 and 3 in Table 3, highlight different approaches to predicting extraction efficiency in a modified spray column. Model 2, achieved an R² of 0.984 and an adjusted R² of 0,954, with a standard error of 0,42 and an F-value of 32.3. in contrast, model 3, showed a slightly lower R² of 0.96 and R² adj. of 0.88, but had a notably lower standard error of 0.081 and an F-value of 12.18. Model 5, was the least reliable, with an R² of 0.907, an Adjusted R² of 0.72, a standard error of 3.912, and an F-value of 4.89, showing lower overall significance and fit compared to the other models.

Model 4:
$$(E\%) = 0.737 Re^{-0.21438} We^{305.6}$$

In this model, Weber number seemed to have significant effect on the efficiency through its high exponent. Thus, interfacial tension around drops played an important role in mass transfer between phases rather than inertial forces represented by Reynolds number. To explain the negative exponent of the Reynolds number in the extraction efficiency correlations, it is well known that higher turbulence, represented by higher Reynolds numbers, results in smaller drop sizes. This is consistent with the physics of fluid breakup where higher inertial forces break the droplets into smaller sizes. Smaller drops can enhance mass transfer rates due to the higher surface area available for transfer. This discussion can interpret the good matching between the predicted and actual values. This is in agreement with Ghorbanian et al., (2011). The predicted extraction efficiency values, by Model 4, versus the actual values are depicted in Fig. 8 which shows a good matching between them that demonstrates the predictive model in estimating extraction efficiency.

5.5. Statistical Analysis of Droplet Size Models

Table 4 summarizes the performance of three models predicting the Sauter mean diameter (d32) based on Reynolds (Re) and Weber (We) numbers. Model 3 exhibited the highest predictive accuracy, highlighting the superiority of predicting d32. Model 3 demonstrated the highest reliability with an R² of 0.999, the lowest standard error of 1.23776E-05, and the highest F-value of 16173.4053, indicating it as the best fit for predicting d32 with the given parameters. Fig. 9 shows the predicted values of d32 with the actual ones. The high degree of alignment between predicted and actual values underscores the reliability and accuracy of the model in predicting the Sauter mean diameter in the given liquid-liquid extraction system.

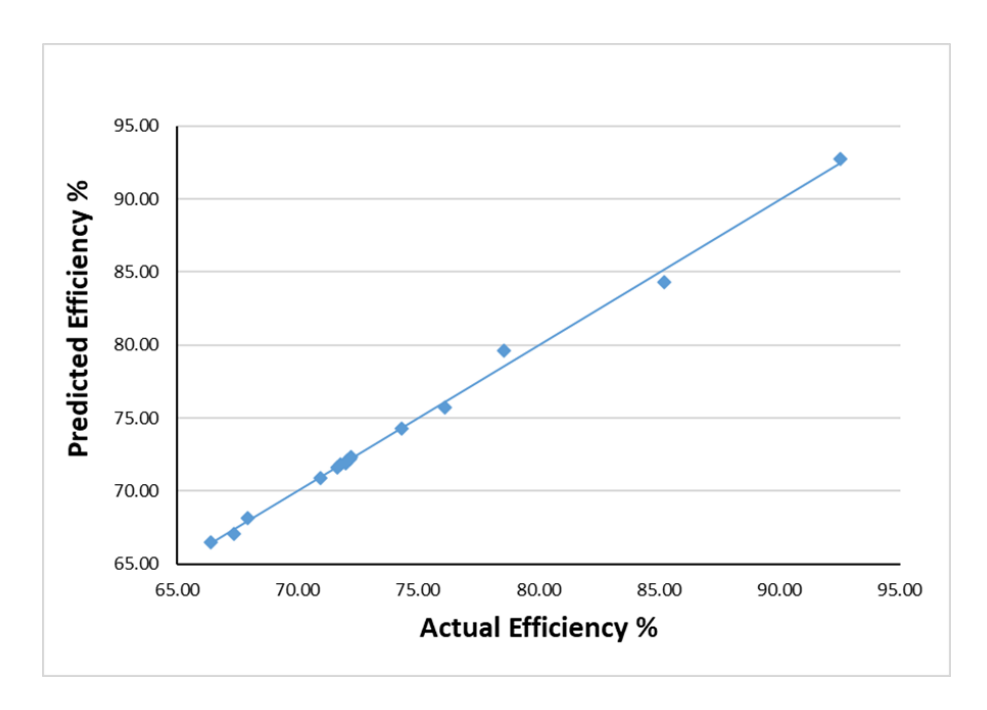


Fig. 8. Predicted Extraction Efficiency E% vs. Actual E%

Model 3:
$$\left(\frac{d32}{dN}\right) = 0.0076 Re^{-0.0002} We^{0.0867}$$

In this model, the two exponents of Weber and Reynolds numbers are fractions that indicate less effect on the Sauter mean diameter. Namely, the designed diameter of the nozzle has the most significant effect. This conclusion is supported by literature by Ghorbanian et al., (2011). Again, the negative sign of the Reynolds number confirmed its reversal effect on the Sauter mean diameter.

Ξ
Ξ
=
\ddot{c}
>
ā
ᅙ
S
Modified S
ij
즂
9
~
Ę.
2
9
Ē
쩅
H
5
\circ
e
p
Ž
<u> </u>
ည
e
:⊇
Effi
Ĭ
ij
ဒ္ဓ
Ë
X
云
3
ž
ap
Ξ

					•		•	•			
	Model		\mathbb{R}^2			t -Stat			P-value		
	$(E\%) = C1 Re^{C2} We^{C3}$	₩	Adj	St.Error	CI	C2	C3	C1	C2	C3	F-value
-	$(E\%) = 0.713 Re^{0.3203} We^{338.26}$	0.986	96.0	1.457	13.84667	0.682495	0.722346	0.045897	0.618741	0.601752	37.87
2	$(E\%) = 0.666 Re^{-0.0703} We^{243.61}$	0.984	0.954	0.42	44.87527	-0.5196	1.80317	0.014184	0.694927	0.322354	32.3
3	$(E\%) = 0.712 Re^{0.03942} We^{-18.93}$	0.960	0.881	0.081	246.5188	1.496266	-0.72012	0.002582	0.375067	0.602684	12.18
4	$(E\%) = 0.737 Re^{-0.21438} We^{305.6}$	0.991	0.975	0.175	118.9443	-3.79412	5.419558	0.005352	0.16406	0.116161	61.39
5	$(E\%) = 0.678 Re^{1.281} We^{-663.4}$	0.907	0.72	3.912	4.9123	1.01701	-0.52774	0.12787	0.49463	0.69086	4.894
		Table 3	. Sauter	Mean Diame	Table 3. Sauter Mean Diameter Model Correlations in Modified Spray Column.	rrelations in N	Iodified Sp	ray Column			
. !	Model		R ²			t -Stat			P-value		
	$\left(\frac{d32}{dN}\right) = C1 Re^{C2} We^{C3}$	\mathbb{R}^2	Adj	St.Error	C1	C2	C3	C1	C2	C3	F-value
1	$\left(\frac{d32}{dN}\right) = 0.0067 Re^{-0.0001145}$	0.985	0.977	0.000191056	26.90732731	-11.56580876		0.00137835	0.00739284		133.767932
7	$\left(\frac{d32}{dN}\right) = 0.00548 \ We^{-0.1104815}$	0.921	0.882	0.000439827	14.96047	-4.85989		0.004438	0.039827		23.61856
8	$\left(\frac{d32}{dN}\right) = 0.0076 Re^{-0.0002} We^{0.0867}$	0.999	0.999	1.24E-05	174.04644	-50.242832	21.806334	0.00365772	0.01266919	0.02917382	16173.4053

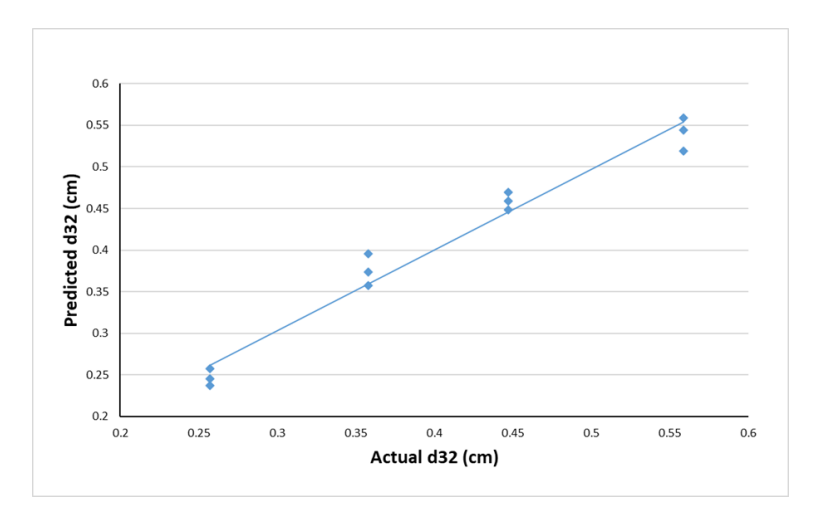


Fig. 9. Predicted Sauter Mean Diameter, d32 vs. Actual d32

Table 5, presents a summary of the Average Absolute Relative Deviation (AARD%) for different models, which is a measure of the accuracy of these models. The AARD% for the d32 model is lowest in model 3 at 0.135%, indicating the highest accuracy for predicting drop size. Model 2, however, shows a higher AARD% at 7.61%, suggesting less accuracy for drop size predictions. For the E% model, Model 3 again demonstrates the lowest AARD% at 0.0496%, confirming its reliability in predicting extraction efficiency. Model 5 has the highest AARD% for the E% model at 1.94%, indicating it is the least accurate among the models evaluated. Models 1 and 4 show intermediate accuracy with AARD% values of 0.782% and 0.106% respectively for the E% model. These results highlight the varying performance of each model in accurately predicting both drop size and extraction efficiency.

Table 5. AARD %

Model	AARD%-d32 model	AARD%-E% model
Mode 1	3.54	0.782
Model 2	7.61	0.271
Model 3	0.135	0.0496
Model 4	-	0.106
Model 5	-	1.94

6. CONCLUSION

A modified (LLE) spray column was designed and constructed to extract aromatic compounds from reformate naphtha using furfural solvent. The effects of the solvent-to-feed ratio and the rotor speed were investigated. The results showed that a limited increase in the S/F ratio enhanced the extraction efficiency. On the contrary, higher rotor speeds generally reduce extraction efficiency due to increased turbulence and phase coalescence, which diminish mass transfer effectiveness. Removing the rotor installation enhanced the extraction efficiency further recording the highest value of 96.5% at 2 S/F ratio. Five mathematical models based on

dimensional analysis were suggested to predict the extraction efficiency and Sauter mean diameter. The statistical analysis showed that Model 4 ($(E\%) = 0.737 Re^{-0.21438} We^{305.6}$) was the most reliable one to predict the extraction efficiency due to its highest F-value and lowest standard error. This model effectively incorporates Reynolds (Re) and Weber (We) numbers, highlighting their importance in predicting extraction efficiency (E%). The correlation between predicted and actual efficiency values shows a strong positive relationship, affirming the accuracy of the predictive models.

Model 3 ($\left(\frac{d32}{dN}\right)$ = 0.0076 $Re^{-0.0002}$ $We^{0.0867}$) exhibited the highest predictive accuracy for d32. This model shows less significant effects of both Weber and Reynolds numbers with the likeliness of being the designed nozzle diameter more effective. The findings emphasize the importance of optimizing operational parameters, such as rotor speed and S/F ratio, to enhance extraction performance. The developed models demonstrate high accuracy and reliability, offering valuable tools for improving LLE processes in industrial applications.

7. REFERENCES

Amani, P., Asadi, J., Mohammadi, E., Akhgar, S. and Esmaili, M., 2017. Cooperative influence of D2EHPA and TBP on the reactive extraction of cobalt from sulfuric acid leach solution in a horizontal semi-industrial column. Journal of Environmental Chemical Engineering, 5(5), pp.4716-4727. https://doi.org/10.1016/j.jece.2017.08.044

Bahadur, I., Singh, P., Kumar, S., Moodley, K., Mabaso, M. and Redhi, G., 2014. Separation of aromatic solvents from the reformate fraction of an oil refining process using extraction by a designed ionic liquid. Separation Science and Technology, 49(12), pp.1883-1888. https://doi.org/10.1080/01496395.2014.900568

Dash, S. and Mohanty, S., 2019. Mathematical modeling aspect in solvent extraction of metals. Separation & Purification Reviews, 50(1), pp.74-95. https://doi.org/10.1080/15422119.2019.1648294

De Lucas, A., Rodríguez, L., Sánchez, P. and Carnicer, A., 1993. Extraction of aromatic compounds from heavy neutral distillate lubricating oils by using furfural. Separation Science and Technology, 28(15-16), pp.2465-2477. https://doi.org/10.1080/01496399308019749

Ferro, V.R., De Riva, J., Sanchez, D., Ruiz, E. and Palomar, J., (2015). Conceptual design of unit operations to separate aromatic hydrocarbons from naphtha using ionic liquids. COSMO-based process simulations with multi-component "real" mixture feed. Chemical Engineering Research and Design, 94, pp.632-647. https://doi.org/10.1016/j.cherd.2014.10.001

Ghorbanian, S. A., Abolghasemi, H., Radpour, S. R. (2011). 'Modelling of Mean Drop Size in a Extraction Spray Column and Developing a New Model', Iranian Journal of Chemistry and Chemical Engineering, 30(4), pp. 89-96. https://doi.org/10.30492/ijcce.2011.6094

Hoseini, S.F., Tavakkoli, T. and Hatamipour, M.S. (2009) 'Extraction of aromatic hydrocarbons from lube oil using n-hexane as a co-solvent'. separation and purification technology, 66(1), pp.167-170. https://doi.org/10.1016/j.seppur.2008.11.027

Idrees, S.A., Mustafa, L.L. and Saleem, S.S., 2019. Improvement viscosity index of lubricating engine oil using low molecular weight compounds. Science Journal of University of Zakho, 7(1), pp.14-17. https://doi.org/10.25271/sjuoz.2019.7.1.572

Karmakar, S., Bhowal, A. and Das, P., 2020. Process Intensification of Liquid-Liquid Extraction in Rotating Packed Bed. In Materials Science Forum. Vol. 998, pp. 146-150. https://doi.org/10.4028/www.scientific.net/MSF.998.146

Kumar, U.A. and Mohan, R., 2011. Liquid—Liquid Equilibria Measurement of Systems Involving Alkanes (Heptane and Dodecane), Aromatics (Benzene or Toluene), and Furfural. Journal of Chemical & Engineering Data, 56(3), pp.485-490. https://doi.org/10.1021/je100908f

Law, J.D. and Todd, T.A., 2008. Liquid-liquid extraction equipment. Hydrometallurgy 42(3), 1247-1252. http://refhub.elsevier.com/S1004-9541(18)31675-6/rf0010

Mahmoudi, J. and Lotfollahi, M.N., 2010. (Liquid+ liquid) equilibria of (sulfolane+ benzene+ n-hexane), (N-formylmorpholine+ benzene+ n-hexane), and (sulfolane+ N-formylmorpholine+ benzene+ n-hexane) at temperatures ranging from (298.15 to 318.15) K: Experimental results and correlation. The Journal of Chemical Thermodynamics, 42(4), pp.466-471. https://doi.org/10.1016/j.jct.2009.10.010

Matar, S. and Hatch, L.F., (2001) 'Chemistry of petrochemical processes', 2nd ed., Elsevier, Gulf Publishing Company, Houston, Texas, USA.

Mehrkesh, A.H., Hajimirzaee, S., Hatamipour, M.S. and Tavakoli, T., 2011. Artificial neural network for modeling the extraction of aromatic hydrocarbons from lube oil cuts. Chemical engineering & technology, 34(3), pp.459-464. https://doi.org/10.1002/ceat.201000361

Mostafa, H.Y., El Naggar, A., Elshamy, E., Farag, A. and Hashem, A., 2019. Utilization of binary mixtures of different solvents for aromatics extraction from a petroleum wax distillate feedstock. Egyptian Journal of Chemistry, 62(9), pp.1749-1759. https://dx.doi.org/10.21608/ejchem.2019.11014.1705

Saien, J. and Jafari, F., 2019. Mass transfer intensification strategies for liquid–liquid extraction with single drop investigations. International Journal of Heat and Mass Transfer, 144, p.118603. https://doi.org/10.1016/j.ijheatmasstransfer.2019.118603

Sakthithasan, P., Orth, L., Venhuis, M. and Kockmann, N., 2023. Design of a Process-Intensified Liquid-Liquid Extraction Cell for Higher Temperature and Pressure. Chemical Engineering & Technology, 46(5), pp.882-890. https://doi.org/10.1002/ceat.202200550

Salimi-Khorshidi, A., Abolghasemi, H., Khakpay, A., Kheirjooy, Z. and Esmaieli, M., 2013. Spray and packed liquid–liquid extraction columns: drop size and dispersed phase mass transfer. Asia-Pacific Journal of Chemical Engineering, 8(6), pp.940-949. https://doi.org/10.1002/apj.1739

Sovilj, M.N., 2012. Hydrodynamics of gas-agitated liquid-liquid extraction columns. Acta periodica technologica, (43), pp.199-216. https://doi.org/10.2298/APT1243199S

Toghyani, M. and Rahimi, A., 2017. Mathematical modeling and parametric study of aromatics extraction from aliphatics with ionic liquids in a rotating disc extractor. Journal of environmental chemical engineering, 5(1), pp.1244-1251. https://doi.org/10.1016/j.jece.2017.02.012

Varfolomeev, B.G., Pebalk, V.L., Chigogidze, K.S., Lan, N.N. and Fernando, R.S., 2000. Spray extraction columns: Drop size and dispersed-phase holdup. Theoretical Foundations of Chemical Engineering, 34, pp.556-561. https://doi.org/10.1023/A:1005220923651